land

Article

Prompt Mapping Tree Positions with Handheld Mobile Scanners Based on SLAM Technology

Juliána Chudá [1], Jozef Výbošťok [1,*], Julián Tomaštík [2], František Chudý [2], Daniel Tunák [2], Michal Skladan [1], Ján Tuček [2] and Martin Mokroš [1,3,4,5]

1 Department of Forest Harvesting, Logistics and Ameliorations, Faculty of Forestry, Technical University in Zvolen, T. G. Masaryka 24, 96001 Zvolen, Slovakia; xchudaj@is.tuzvo.sk (J.C.); xskladan@is.tuzvo.sk (M.S.); m.mokros@ucl.ac.uk (M.M.)
2 Department of Forest Resources Planning and Informatics, Faculty of Forestry, Technical University in Zvolen, T. G. Masaryka 24, 96001 Zvolen, Slovakia; tomastik@tuzvo.sk (J.T.); chudy@tuzvo.sk (F.C.); tunak@tuzvo.sk (D.T.); tucek@tuzvo.sk (J.T.)
3 Faculty of Forestry and Wood Sciences, Czech University of Life Sciences, 165 21 Prague, Czech Republic
4 Department of Geography, University College London, Gower Street, London WC1E 6BT, UK
5 NERC National Centre for Earth Observation (NCEO), University College London, London WC1E 6BT, UK
* Correspondence: jozef.vybostok@tuzvo.sk

Abstract: In this study, we evaluated the performance of GeoSLAM ZEB Horizon and Stonex X120GO SLAM handheld mobile laser scanners (HMLS) to address two primary objectives. First, we aimed to assess and compare the accuracy of positioning achieved using HMLS instruments. Second, we sought to investigate the influencing factors and their impact on estimation accuracies. The factors influencing the accuracy of positioning in HMLS Simultaneous Localization and Mapping-aided solutions were defined, considering the scanner type, distance from the trajectory, forest structure, tree species, and Diameter at Breast Height. The same type of trajectory was tested in five different stand structures. The evaluation of GeoSLAM HMLS point clouds yielded an average positional RMSE of 17.91 cm, while the data extracted from the Stonex HMLS resulted in an average positional RMSE of 17.33 cm. These results underscore the significant potential of HMLS technology in addressing the critical need for precise positioning data in various applications, from forestry management to environmental monitoring, wildlife habitat assessment, and climate change studies. By harnessing the power of handheld mobile laser scanners, our research aims to enhance the accuracy and efficiency of geospatial data capture in challenging.

Keywords: position; SLAM; tree; mapping; forest

check for updates

Citation: Chudá, J.; Výbošťok, J.; Tomaštík, J.; Chudý, F.; Tunák, D.; Skladan, M.; Tuček, J.; Mokroš, M. Prompt Mapping Tree Positions with Handheld Mobile Scanners Based on SLAM Technology. *Land* **2024**, *13*, 93. https://doi.org/10.3390/land13010093

Academic Editor: Todd Robinson

Received: 25 November 2023
Revised: 2 January 2024
Accepted: 11 January 2024
Published: 13 January 2024

Copyright: © 2024 by the authors. Licensee MDPI, Basel, Switzerland. This article is an open access article distributed under the terms and conditions of the Creative Commons Attribution (CC BY) license (https://creativecommons.org/licenses/by/4.0/).

1. Introduction

Precise geospatial data plays a key role in enabling a comprehensive understanding of location, distance, and area within society, while in the domain of forestry, the widespread adoption of global navigation satellite system (GNSS) based positioning tools facilitates effective navigation and assist the management decisions [1]. Tree position plays an important role in research on forest resources and ecological functions, and quickly and accurately obtaining tree position data has long been the focus of researchers. The rapid and accurate acquisition of tree position in sample plots is helpful for predicting the growth of tree diameter at the breast height (DBH) and population development trends and has important ecological significance for revealing the relationship between trees and tree species [2]. Accurate tree positioning and measurement of structural parameters are the basis of forest inventory and mapping. Also, they are important for forest biomass calculation and community dynamics [3]. The structure and diversity of a forest may be defined by the spatial distribution of the tree positions, by the particular mingling patterns of the different tree species that occur in the forest and by the spatial arrangement of the tree dimensions [4]. The position plays a significant role in modeling individual-tree growth and survival, identifying the vertical structure, and growth pattern of trees in the forest and forms topography.

In early days, the location of sample trees was mainly surveyed in the horizontal distance by means of compass angle, tape, or lining rope [5], which was very time consuming. More precise technologies that could be used in forestry began to emerge later. Only recently methods and devices have been developed for locating trees in challenging environments. The global navigation satellite system (GNSS) can provide positioning coordinate information in most environments. However, in forested areas with high canopy cover index and diverse tree densities within sample plots, GNSS signals may experience signal attenuation or disappearance, impacting positioning accuracy [2]. Many factors, including dilution of precision, multipath errors, atmospheric refraction, clock errors, and ephemeris errors, can affect the quality of GNSS data in complex environments. To address this, researchers explore possible combinations GNSS with other technologies, such as inertial measurement units (IMUs), to achieve sub-meter accuracy in challenging forest conditions, benefiting applications like accurate forest mapping and object positioning [6,7]. Recent advancements in technological combinations, including complex fusions of devices, have enabled achieving accuracies of less than 0.5 m in challenging forest environments [8–12]. Therefore, it is necessary to investigate new possibilities and pathway patterns that will allow the accuracy of determining the location of objects in a challenging environment to be increased. For the purposes of forest inventory data collection, authors used to work with Field-Map system, a software and hardware technology for computer-aided field data collection and data processing that combines a real-time GIS software with electronic equipment for mapping and dendrometric measurements [13–16]. However, accurate location estimation is not among its primary goals and the position is estimated with a high error.

Advancements in consumer mobile mapping technologies have enabled easy collection of geospatial data from challenging environments, both indoors and outdoors, using laser scanning and powerful computational devices [17]. These laser scanning techniques provide detailed and accurate environmental images, where the accuracy of locating objects is dependent on the quality of input data, with some drawbacks of high time consumption and cost. Terrestrial laser scanners (TLS) are widely used in obtaining 3D representations of an environment and achieve good accuracy. Their disadvantages have already been mentioned (time consumption, speed, and equipment acquisition costs).

Handheld mobile laser scanners emerged as an alternative to TLS around 2013, offering higher efficiency and promising applications in forestry [18,19]. Leveraging Simultaneous Localization and Mapping (SLAM) technology, these scanners provide detailed and relatively accurate environmental point clouds and enable efficient and accurate object positioning, making them valuable tools in various industries, including forestry [7]. The use of mapping techniques based on SLAM as a more favorable alternative to traditional static mapping methods in a complicated environment was described in [20]. SLAM is a process where a mobile robot simultaneously creates a map of its environment and determines its own position using this map. It involves estimating the robot's trajectory and the locations of all landmarks in real-time, without relying on any prior knowledge or pre-existing maps [21]. That means SLAM technology does not inherently rely on a GNSS signal, making it advantageous for use in environments where GNSS signals are unavailable.

Several works investigate the applications of mobile laser scanners and SLAM technology in various industries, including forestry [20,22–24]. With the development of indoor applications of mobile robotics, the popularity of the technology is increasing. It is also an interesting alternative solution for creating maps for different and specific purpose in various industries [25]. In the application of SLAM technology for the forest environment, research has been moving forward in recent years.

The first commercial handheld mobile mapping system powered by a smart algorithm was developed by the GeoSLAM team [26,27]; later, several companies began to develop the technology of mobile scanners, and more affordable devices began to appear, enable wider application in practice for forest inventory or natural conditions monitoring (in 2014 Google released "Project Tango" [28,29] or Intel's RealSense handheld 3D mapping technology [30]).

SLAM is a longstanding challenge in mobile robotics and artificial intelligence, studied extensively for more than two decades. Researchers employ diverse techniques to enhance robot autonomy and self-navigation. Autonomous robots require a deep understanding of their environment and the ability to navigate in unknown territories. This is vital, especially in indoor settings where GNSS is unavailable. Researchers continue to develop improved SLAM techniques to ensure reliable and efficient robot navigation, making it a practical and essential technology with a wide range of applications in both indoor and outdoor environments [31]. Hence, it is crucial to explore the capabilities of devices employing this technology in challenging environments and validate the data from manufacturers' technical specifications through real-world practical testing.

Recently, the Stonex X120GO SLAM appeared as a possible alternative tool for 3D point cloud acquisition, potentially replacing the Geo SLAM ZEB Horizon. A series of studies has delved into the use of handheld and mobile laser scanning technologies for a range of applications. Researchers have explored the potential of mobile handheld laser scanners in assessing external structures influencing the quality of wood in trees [32]. These technologies have been employed to compare various scanning approaches, including SLAM-based HMLS called TORCH, and close-range terrestrial photogrammetry for measuring surface deformation on forest roads [33]. Garden settings have been the subject of extensive laser scanning studies, evaluating both static TLS and mobile laser scanning (MLS), utilizing equipment such as the Focus 3D S120 and the Leica BLK2GO [34]. A mixed-species Mediterranean forest was used as the testing ground for estimating individual tree attributes with HMLS [35]. Furthermore, 3D laser scanning data from SLAM-based portable sensors have been tested for cadastral surveys in complex urban areas [36]. These advanced technologies have been applied for documenting intricate architecture [37]; additionally, HMLSs have gained attention for documenting cultural heritage in various urban environments [38]. Additionally, authors often compare HMLSs with various technologies, such as TLS, airborne laser scanning (ALS), photogrammetry, or other remote sensing outputs [39–42], but, to the best of our knowledge, no one has yet compared these two devices and their precision and limits in forests environment.

The main goal of this study is to compare the accuracy of individual devices in terms of positional accuracy and to look for factors that influence this error. In addition, we investigate the possibilities of two different HMLSs with SLAM technology in challenging environment of forest stands with different structure, including the device with a long-standing tradition (GeoSLAM) and the new more affordable Stonex device. Comparing two different HMLSs in a challenging environment can be beneficial for several reasons, primarily in evaluating performance, assessing data quality, and identifying potential issues. This study assessed the scanners' performance and capabilities, compared their performance, and easily outlined cost-effectiveness, which can help individuals and organizations make informed decisions when selecting the most suitable scanner for their specific needs. Our comparisons of devices provide a benchmark for understanding the relative performance of these devices, enabling users to gauge which SLAM HMLS offers better results or reliability in challenging environments. This is crucial in various applications like forestry, architecture, archaeology, or surveying, where data accuracy is paramount.

Accuracy of forest inventory data collection with emphasis on individual tree position will be evaluated. The factors that affect the accuracy of positioning HMLS SLAM-aided solutions will be defined. Overall, understanding how different forest types impact the performance of HMLS systems is crucial for accurately interpreting and utilizing laser scanning data in forest environments. In addition, it is important to determine that the

HMLS position error achieved is not an obstacle to being able to derive important tree, stand, and environmental parameters.

2. Materials and Methods

Test plots are in the middle of Slovakia (Central Europe), in the forest stand of the University Forest Enterprise of the Technical University in Zvolen. Five test plots with dimensions of 30 × 30 m^2 were established and permanently marked with steel survey markers (Figure 1). We selected areas with flat terrain while ensuring they met our retrains.

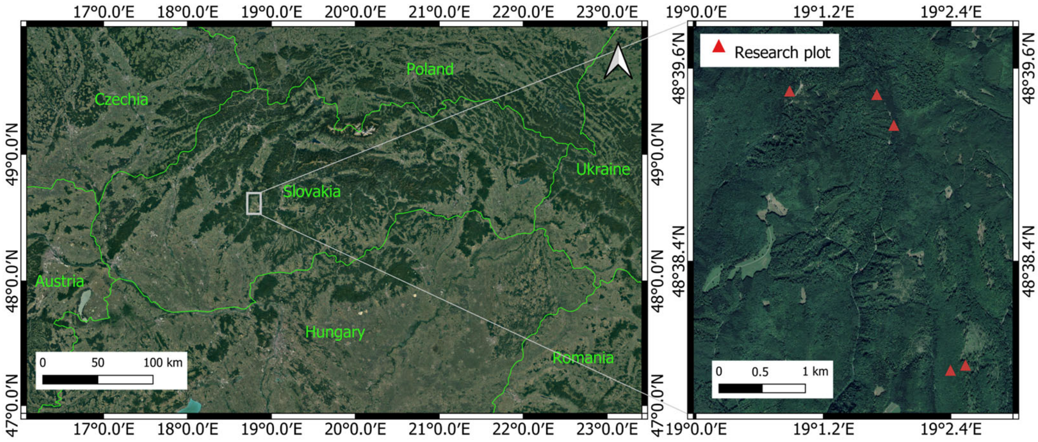

Figure 1. Location of the research plots.

We began data collection in March 2022, marking the start of the leaf-on season in our region. Plots were measured from March to November 2022. We collected reference data initially and then scanned the stands while striving to maintain consistent collection conditions across all research plots. Within each test plot, all trees with a DBH > 2 cm were accurately positioned, using the Topcon 9000 total station combined with the Topcon Hiper SR GNSS receiver (Topcon Corporation, Tokyo, Japan), and the diameters of trees were measured at the height of 1.3 m above the ground using measuring tape (Ben Meadows Co., Madison, WI, USA). All reference data and ground control points (GCPs) positions were collected in the System of the Unified Trigonometrical Cadastral Network coordinate system. The first corner of the research area represents the first position of the total station with additional measurements to at least two known points obtained by post-processed GNSS baselines with base station data obtained from Slovak real-time positioning service (SKPOS®, Bratislava, Slovakia). To measure all the trees on the research area, it was necessary to change the position of the total station several times in denser stands, while the orientation was carried out each time to the known corner points of the research plots. The corner points of the research plots were permanently stabilized by geodetic anchors. The polar method and angular offset were used to determine the position of the trees. The method records the horizontal angle and the distance of the object from the connection point of the total station position and the orientation point—from the known direction with the zero value of the horizontal angle. Each distance of the tree from the device was adjusted by 1/2 DBH during office work to ensure the exact location of the point in the center of tree. The accuracy of determining the position of the corner GCP and tree positions was below the limit of 3 cm. The reference data set was created in compliance with the legislation in force in the field of forest mapping. In the Slovak Republic, two main laws have influenced forest mapping (Slovak Technical Standards—STN; 1. Geodetic points and 2. Charts with scales 1:200, 1:250, 1:500, 1:1000. General and special charts). Essentially, the standards define the classes of accuracy valid for the geodetic control points, which are used as a base for calculation of the other consequential objects-representing points. The fifth class of accuracy is used in the field of forestry, which is brought about by GNSS decreasing effects of forest stands. However, the reference data set was collected with the aim to reach at least the third class of STN—Geodetic control points—with the highest allowed error being 0.06 m [43]. Site conditions are shown in Figure 2. The research areas include different structured stands and are dominated by European beech (*Fagus sylvatica* L.) and Norway spruce (*Picea abies* (L.) Karst.). Research plots include 37 to 166 trees with an average DBH from 16.07 to 29.25 cm (based on our measurements).

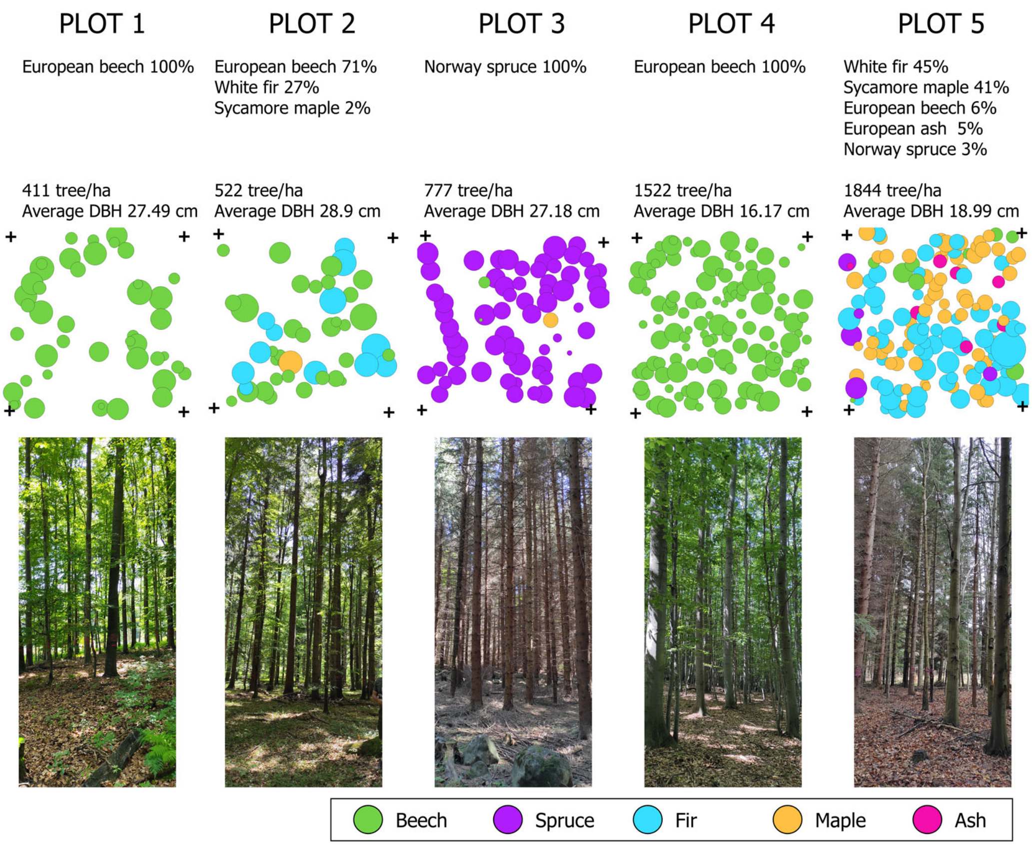

Figure 2. Research plots—situation maps based on reference data measurements.

For a better illustration of the conditions at the research plots average DBHs can be found in Table 1. The research areas contained deciduous and coniferous trees, in various degrees of mixing.

The data acquisition by HMLSs were performed using a GeoSLAM Horizon scanner (GeoSLAM Ltd., Nottingham, UK) and Stonex X120GO SLAM Laser Scanner (Stonex® Srl., Paderno Dugnano, Milan, Italy). According to producers' data both GeoSLAM ZEB Horizon and Stonex X120GO SLAM offer high-quality handheld scanning capabilities with similar relative accuracy and collection rates (Table 2). In the user sector, the choice between the two may depend on specific project requirements, price, user preferences, and the interface or software that best aligns with the user's workflow.

The research areas were scanned continuously in four parallel lines with 10 m distance between each other. This measurement method was chosen to obtain a high density of points and time efficiency. Used HMLS systems captured GCPs using the reference plate accessory. Scanning always started in the lower left corner and proceeded along the lines at 10-m intervals. Both HMLSs required static initialization in the first step. The devices were moved at a uniform speed over the research area, maintaining a 10-m gap between individual lines (Figure 3). For easier orientation and adherence to the scanning scheme, we used simple markers placed beyond the border of the research area.

Table 1. Research plots summary information.

Plot	Age (Average) *	Average DBH **	Number of Trees (Overall) *	Density * (Tree/ha)	Species **	Tree Species Composition (%) **
1	85	27.49	37	411	European beech (*Fagus sylvatica* L.)	100
2	80	28.9	47	522	European beech (*Fagus sylvatica* L.)	71
					White fir (Abies alba Mill.)	27
					Sycamore maple (*Acer pseudoplatanus*)	2
					European ash (*Fraxinus excelsior*)	0
					Norway spruce (*Picea abies* (L.) H. Karst.)	0
3	60	27.18	70	777	Norway spruce (*Picea abies* (L.) H. Karst.)	100
4	65	16.17	137	1522	European beech (*Fagus sylvatica* L.)	100
5	40	18.99	166	1844	White fir (Abies alba Mill.)	45
					Sycamore maple (*Acer pseudoplatanus*)	41
					European beech (*Fagus sylvatica* L.)	6
					Sycamore maple (*Acer pseudoplatanus*)	41
					European Ash (*Fraxinus excelsior*)	5
					Norway spruce (*Picea abies* (L.) H. Karst.)	3

* Data taken from ISLHP (nlcsk.org) © NLC Zvolen; "https://gis.nlcsk.org/islhp/mapa (accessed on 14 September 2023)"; ** Measured at the plot.

Table 2. Technical specifications handheld mobile laser scanners.

Technical Specification	GeoSLAM ZEB Horizon	Stonex X120GO SLAM
Range	100 m	120 m
Laser	Class 1/λ 903 nm	Class 1
FOV	$360^\circ \times 270^\circ$	$360^\circ \times 270^\circ$
Scanner points per second	300,000	320,000
Processing	Post	Post
No. of sensors	16	-
Relative accuracy	Up to 6 mm	6 mm
Scanner weight	1.45 kg	1.6 kg
Datalogger weight (incl. battery)	1.4 kg	-
Colorized point cloud	supported	supported
Protection class	IP 54	IP 54
Operating time	Approximately 3 h	2.5 h (1 battery set—4 pieces)
Mobile app	no	yes
Price (Approximately)	€41,000	€26,400

Based on the manufacturer's description.

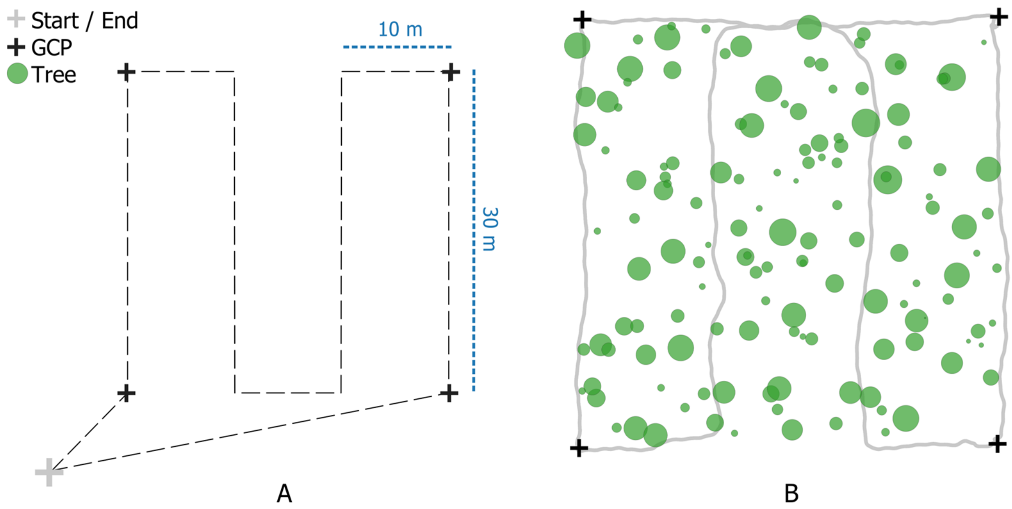

Figure 3. The HMLS data acquisition process; (**A**)—scheme, (**B**)—data collection path.

During the data acquisition process, four GCPs were recorded, one in each corner of the test plot. GCPs were measured by keeping the HMLS stationary for 5–10 s during a scan, and these GCPs were subsequently recognized during the processing stage. The data acquisition in one plot, including scanning and uploading 4 GCPs, did not exceed 10 min (Figure 4). At the end of the scanning, the HMLS was always placed at the same place as at the beginning of work.

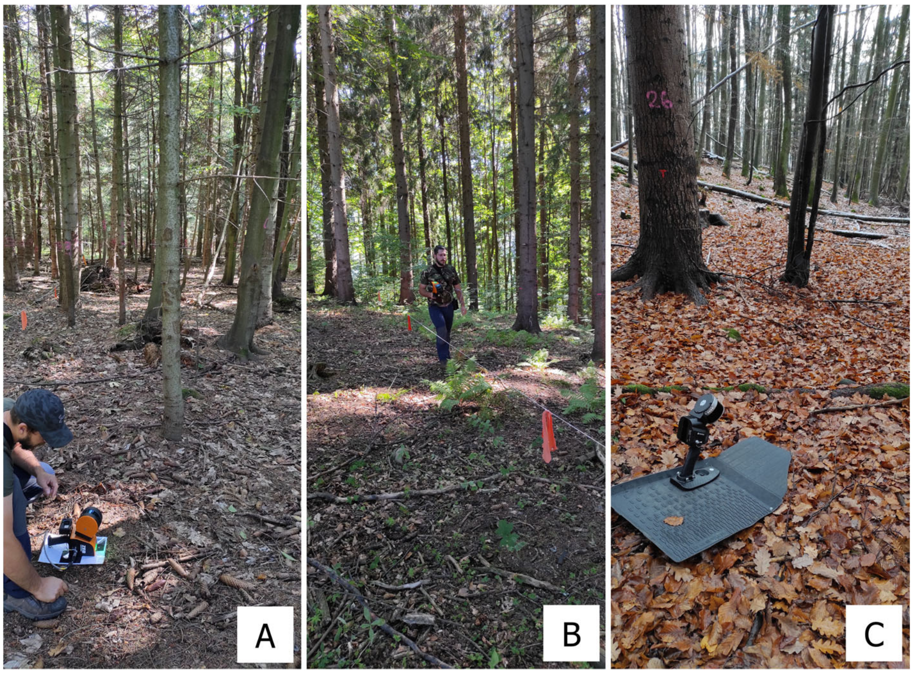

Figure 4. The HMLS's data collection; (**A**)—initialization of GeoSLAM ZEB Horizon; (**B**)–HMLS in work process; (**C**)—Stonex X120GO SLAM initialization.

GeoSLAM Horizon scanner has a collection rate of 300,000 points per second, a relative accuracy of 6 mm, and a range of 100 m, based on the manufacturer's description. It is controlled by a button directly on the scanner, and a cable connection to the datalogger and batteries are required. For GCPs measurement, it is only necessary to remain in a stationary position on the GCP for a few seconds. For the post-processing of scanned data, GeoSLAM Hub software (ver. 5.3.1) was used. During processing in GeoSLAM Hub, we used default parameters and workflows. Subsequently, point clouds from each research area were georeferenced into the national JTSK system (EPSG 5514) using GeoSLAM Draw software (ver. 3.1).

Stonex X120GO SLAM Laser Scanner has a collection rate of 320,000 points per second, a relative accuracy of 6 mm, and a range of 120 m. It uses an RGB camera with a resolution of 5 MPx and a viewing angle of 200° × 100°; as a result, the scanner can color point clouds. It is controlled by the GO app where scans are updated and displayed simultaneously, and it was possible to see the progress of scanning directly in the mobile phone. In this case, it is necessary to stay a few seconds in a stationary position on the GCPs and, at the same time, to record the GCPs in the app. In the field, the GO app was used to control the device and to check and manage projects. For the post-processing of scanned data, the GOpost 1.0.5. software was used. During processing, we used default parameters and workflow.

Nowadays, there is a multitude of open-source software applications available for lidar data segmentation, visualization, measurement, and exporting various tree parameters (e.g Simpletree [44], CompuTree [45], 3DForest [46], 3DFin [47], or DendroCloud [48]. In this study, the position of the trees were detected by the Forest Structural Complexity Tool (FSCT) [49], which allows research area measurements to be extracted automatically from most high-resolution forest point clouds from a variety of sensor sources (TLS, MLS, and ALS).

The FSCT extracts and generates detailed outputs such as fundamental measurements of the trees (coordinates of the tree, DBH, tree height, tree volume, indicator of stem coverage completeness), images presenting straightforward point cloud outputs, and point cloud outputs (various classified and segmented point clouds—terrain, vegetation, stems, etc.).

The subsequent analysis was focused on calculating the distances between individual trees and the trajectory of HMLSs. There is an assumption that the location of the object relative to the HMLS trajectories will affect the result. However, in a complex environment such as forest stands, it is quite difficult to define the share of the influence of surrounding objects on the correct recording of the object of interest (shading by surrounding objects, possible movement of objects in lower layers of the stand, etc.) without interfering with the algorithms in the devices used. For this reason, we decided to calculate the mentioned distances between all objects and subsequently consider and describe the minimum, maximum, and average distances of objects from HMLS trajectories. These values were calculated for each data collection session in all research plots between the trajectory and the reference dataset. The average distance of each tree from the trajectory of the HMLSs provides insights into the magnitude of positional deviations. To facilitate the analysis, linear distance matrices were prepared for both the reference positions of trees within the research areas and the trajectories of both HMLSs. Prior to this step, we reduced the number of points along each trajectory from approximately 28,000 to include a point every 10 cm, thereby reducing the total number to approximately 1000 points per trajectory. The outcome of this process yielded a dataset comprising distances of each tree from the HMLS trajectory. We examined the minimum, maximum, and average values of these distances to better understand the influence of distance between tree and HMLSs trajectory.

Accuracy Assesment

We compared the estimation of position obtained by point clouds with the traditional manual field measures. For each pair of points, the difference in the direction of the axes was calculated in the first step. The position estimation error was computed as the difference between the estimated coordinates (x_{est}, x_{est}) and the reference coordinates (x_{ref}, y_{ref}). To assess the accuracy of the tree-level positional estimations we calculate Euclidean distance between reference and HMLS estimated tree position as follows:

$$distance = \sqrt{\left(x\,dif^2_{(x_{ref}-x_{est})} + y\,dif^2_{(y_{ref}-y_{est})}\right)} \quad (1)$$

In addition, we calculated the *RMSE* as follows:

$$RMSE = \sqrt{\frac{\sum_{i=1}^{n}\left(x_{ref} - x_{est}\right)^2}{n}} \tag{2}$$

where:

- n is the number of data points in the dataset.
- x_{ref} (y_{ref}) is the true (observed) value of the target variable for the i-th data point.
- x_{est} (x_{est}) is the predicted value of the target variable for the i-th data point.
- The summation $\sum_{i=1}^{n}$ goes through all data points and calculates the squared difference between the true and predicted values for each data point.

To evaluate the factors that affect the accuracy of positioning SLAM-aided solutions the following methods of evaluation were used.

The Kruskal–Wallis test [50] was utilized to compare the medians of positioning error across different forest types, allowing us to determine whether there were significant differences in accuracy based on the density of individuals in each forest. That means to find out if there is a difference in the positional error across areas that are made of different tree species.

The independent samples t-test was employed to compare the average positioning error between two distinct HMLS devices, allowing us to determine if there were significant differences in accuracy between the devices.

We used Pearson's correlation [51] for the estimation of influence between the scanner's trajectory data and the accuracy of tree position. Correlations results can indicate a relationship between the positional error and the distance between the tree and the HMLS trajectory.

3. Results

The procedure allowed the evaluation of 417 trees from 457 individual trees. The reference dataset was measured via traditional survey and forest inventory methods. The experimental data consists of point clouds produced by GeoSLAM and Stonex (HMLSs working with SLAM technology). SLAM technology in its essence does not need a GNSS signal; this is the reason why it is advantageous to apply it even in an environment where GNSS is absent. On the other hand, in our work we presented a methodology that is a kind of geodetic basis (transformation into a coordinate system using four known points) in combination with SLAM technology in a complex environment; thus we demonstrate that it is possible to achieve interesting results with good positional accuracy in an affordable way.

3.1. Positional Accuracy and Scanner Influence

The RMSE values for the positioning based on GeoSLAM and Stonex data are presented under various tree density scenarios. Table 3 provides insights into the comparative accuracy and highlights their performance differences in various dimensions (X, Y, and Distance) for each specific density and the overall dataset. Comparable results in terms of distance RMSE were observed between the two HMLSs instruments. An average positional RMSE of 17.91 cm was reached from the GeoSLAM HMLS point clouds evaluation, and 17.33 cm from the data extracted from the Stonex HMLS. Overall, the Stonex device shows a smaller positional error. The results differ the most in the mixed stand with a density of 1552 individuals per hectare and an average DBH of 18.99 cm (Plot 4). In the case of both devices, the highest RMSE value was recorded in the spruce forest stand with a density of 777 trees/ha and an average DBH of 27.18 cm (Plot 3).

Table 3. The accuracy of the HMLSs GeoSLAM Horizon and Stonex X120GO SLAM in estimating tree positions (Unit: cm). Red represents the highest value, and green represents the lowest.

RMSE	GeoSLAM			Stonex			Density (Tree/ha)
	x	*y*	Dist.	*x*	*y*	Dist.	
Overall	**12.67**	**12.65**	**17.91**	**12.89**	**11.58**	**17.33**	
Plot 1	13.08	11.26	17.26	13.25	10.63	16.98	411
Plot 2	6.46	8.04	10.31	6.20	7.18	9.49	522
Plot 3	16.68	13.49	21.45	17.27	13.47	21.91	777
Plot 4	12.90	10.62	16.71	12.18	10.75	16.25	1522
Plot 5	11.88	14.96	19.10	12.31	12.87	17.81	1844

Overall, Table 3 provides a concise representation of how the positioning errors vary between Stonex and GeoSLAM across different distance intervals. In the 0–5 cm distance range (Figure 5). Stonex and GeoSLAM exhibit similar percentages for *x*, *y*, and overall distance differences, with Stonex having a slightly higher percentage in the *y*-axis category. As the distance range increases, the percentage of points acquired in *x* and *y* axes tends to show a gradual decrease for both devices. In the higher distance ranges (26–30 cm, 31–35 cm, and 36+ cm), GeoSLAM seems to consistently outperform Stonex in terms of the proportion of points with smaller errors in both x and y axes. Graphical visualization in Figure 5 indicates that GeoSLAM performs relatively better than Stonex for larger distances, which might be valuable information for selecting the appropriate positioning method based on the required accuracy and distance range.

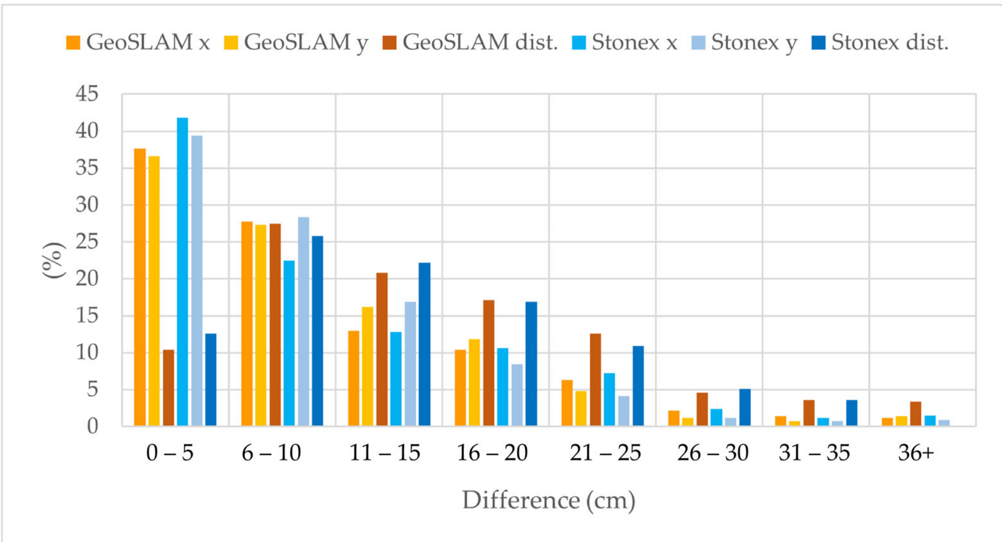

Figure 5. The graphical representation of error distribution. Within each interval, the percentages represent the proportion of data points falling within that range for both the *x*-axis, *y*-axis, and overall distance.

3.2. Influence of Distance from the Trajectory

Due to a more complex view of the research study, the distances of the trees from the trajectory of both devices were calculated according to the procedure described in the previous part of the study. For both HMLS approaches, the maxima occur in the same stand types—mixed stand and spruce stand with high density of individuals per hectare. GeoSLAM exhibits slightly higher average distances (*x*: 9.59 cm, *y*: 9.63 cm, distance: 15.13 cm) than Stonex (*x*: 9.65 cm, *y*: 8.89 cm, distance: 14.65 cm) in both x and y coordinates and overall distance (Table 4). GeoSLAM exhibits higher average distances than Stonex in all dimensions for plot with density of 1522 trees/ha (young beech forest stand). In a density of 411 trees/ha, GeoSLAM demonstrates slightly higher average distances in the *x* and *y* coordinates, but similar average overall distances (old beech forest). In a spruce tree forest with a density of 777 trees/ha, GeoSLAM has higher average distances than Stonex in both x and y coordinates and overall distance. In mixed stands with densities of 522 and 1844 trees/ha, GeoSLAM shows higher average distances compared to Stonex in the y and overall distance dimensions for lower density and demonstrates slightly higher average distances than Stonex in all dimensions for higher density. The largest maximal distance between trees and the trajectory can be seen at the data from the plot with a mixed stand and a density of 1844 trees/ha. For the largest average distance, we could look at the values from spruce plot with density of 777 trees/ha. This is due to the shape of the trunk specific to spruce, which is branched almost from the base of the trunk.

Table 4. Distances of trees from the trajectory of GeoSLAM and Stonex (Unit: m). Red represents the highest values.

	GeoSLAM									
		x			***y***			**Distance**		**Density (tree/ha)**
	MIN	**MAX**	**AVG**	**MIN**	**MAX**	**AVG**	**MIN**	**MAX**	**AVG**	
Overall	**0**	**54.1**	**9.59**	**0**	**56.7**	**9.63**	**0**	**61.49**	**15.13**	
Plot 1	0.17	32.62	11.07	0	41.2	8.86	3.28	45.59	15.41	411
Plot 2	0.15	17.76	4.61	0	26.8	5.96	0.65	31.41	8.21	522
Plot 3	0.09	42.6	12.12	0.3	39.99	10.6	1.53	42.95	18.01	777
Plot 4	0.5	31.7	9.62	0.2	32.7	8.51	1.92	33.11	14.81	1522
Plot 5	0	54.1	8.73	0.09	56.7	11.46	1.99	61.49	16.28	1844
	Stonex									
		x			***y***			**Distance**		**Density (tree/ha)**
	MIN	**MAX**	**AVG**	**MIN**	**MAX**	**AVG**	**MIN**	**MAX**	**AVG**	
Overall	**0**	**54.6**	**9.65**	**0**	**52.9**	**8.89**	**0**	**59.64**	**14.65**	
Plot 1	0.53	31.51	11.05	0.09	39.8	8.37	1.82	44.79	15.15	411
Plot 2	0.03	17.34	4.59	0	25.6	5.22	0.2	29.68	7.56	522
Plot 3	0.19	45.3	12.33	0.3	36.59	10.56	1.58	45.51	18.37	777
Plot 4	0	30.39	9.08	0.09	34.69	8.63	1.03	35.52	15.15	1522
Plot 5	0.19	54.6	9.06	0.2	52.9	9.92	1.93	59.64	15.1	1844

We utilized Pearson correlations to explore the relationship between the distance of the tree from the HMLS trajectory and the size of the positioning error. The resulting correlation coefficients revealed relatively small values, predominantly around 0.2 or lower, indicating the presence of weak correlations between the tree distance from the trajectory and the error size. According to the previous results, the distance from the trajectory does not affect the positioning error.

3.3. Influence of Forest Structure

Testing the influence of the plot (density) on the position error was tested with the Kruskal–Wallis test; this showed that there is a statistically significant difference between the plots regarding the error. Thus, forest density affects the positional error. When comparing the size of the positional error between the mentioned location and all other results from the research areas, a statistically significant difference was observed and a statistically significant difference in the size of the individual's location error was demonstrated.

The distance between reference tree position and position calculated from point cloud from Stonex and GeoSLAM were tested. Based on the investigation, it was demonstrated that, in the case of both HMLSs, a statistically significant difference was recorded to a greater extent in connection with the error on the *x* axis. Regarding HMLS GeoSLAM, statistical significance was observed in five cases when examining the *x*-axis, and only in two cases when examining the *y*-axis. With HMLS Stonex, the *p*-value exceeded the significance level in four cases in connection with the x-axis and in three cases with the y-axis.

For the X-axis, the significance level was exceeded by both HMLS systems when comparing a mixed stand with a density of 522 trees/ha with stands having densities of 1844 trees/ha, 777 trees/ha, and 1522 trees/ha. Similarly, statistical significance was observed when comparing a mixed stand with a density of 1844 trees/ha with a beech stand having a density of 1552 trees/ha and average DBHs of 18.99 cm and 16.17 cm, respectively.

The difference was displayed in the data from HMLS GeoSLAM, where the p-value exceeded the significance level when examining the error in stands with a similar structure and number of individuals. Specifically, this was evident when comparing a mixed stand with a density of 522 trees/ha and an average DBH of 28.9 cm with a beech forest having a density of 411 trees/ha and an average DBH of 27.49 cm.

The statistical significance of the type of plot affecting the position error was displayed in the direction of the Y-axis only when comparing a mixed stand with a density of 522 trees/ha and plot densities of 1844 trees/ha (mix plot), and 777 trees/ha (spruce plot) in HMLS GeoSLAM data evaluation. With HMLS Stonex, the p-value dropped below the value of 0.05 even at a density of 1552 trees/ha.

The varying tree densities, local mixing in the mixed forests, and canopy structures in young plots present distinct challenges for data collection and contribute to the differences in positional error on the X-axis. Additionally, the specific characteristics of each HMLS system may also interact differently with the diverse forest conditions, further influencing the observed results. For example, the high noise in Stonex data may relate to strong p-values in the influence of forest structure testing when comparing an old mixed forest with a density of 522 trees/ha with all plots situated in a young forest with a higher density of trees per hectare.

3.4. Influence of Tree Species

The influence of tree species on positional error was examined, and it was found that tree species significantly affect the error, except for the x-axis error, in Stonex data. Specifically, when analyzing the errors along the y-axes, Stonex showed statistically significant differences between fir and maple (p-value = 0.036) and between beech and maple (p-value = 0.03). On the other hand, for the x-axis errors in GeoSLAM data, statistically significant differences were observed between fir and beech (p-value = 0.014) and fir and spruce (p-value = 0.024). Furthermore, when evaluating the y-axis errors in GeoSLAM data, there were significant differences between fir and maple (p-value = 0.002) and between beech and maple (p-value = 0.000).

These findings show that the tree species composition can have a substantial impact on the positional error in HMLS data, highlighting the importance of considering tree species when analyzing and interpreting such data in forest environments. The influence of the tree species on the positioning error was demonstrated in all cases, except for the x-axis with the Stonex device.

The observed influence of tree species on positional error can be attributed to the inherent variations in tree morphology and bark characteristics among different species and ages. Coniferous and deciduous tree species exhibit distinct differences in their growth patterns, which can impact the accuracy of positioning based on HMLS. Furthermore, the distinct bark textures and colors of different tree species can also impact laser reflection and absorption.

Additionally, tree species also vary in their growth rates and overall size. Younger trees of certain species may have different canopy structures and branch arrangements compared to older, more mature trees. These differences can affect the laser beam penetration and the resulting point cloud data, contributing to variations in positional error (lower branching, twigs at the base of the trunks, branch shoots, etc.).

3.5. Influence of Diameter at Breast Height

The Pearson's correlations showed that there is no correlation between position determination error and DBH or DBH determination error (Table 5 (a)). The diameter of the tree does not affect the position error; in other words, there is no more significant position error on thick trees than on thin ones. When examining the relationship between position error and thickness error (Table 5 (b)), we aimed to determine whether trees with inaccurately determined positions also exhibit inaccuracies in DBH. However, the correlation between these two variables was not confirmed. In other words, the error in DBH is not necessarily related to the position error. Consequently, a significant position error does not necessarily imply a significant DBH error.

Table 5. DBH and DBH determination error correlation coefficients.

	(a) DBH	(b) DBH Error
Stonex		
x	0.124	0.084
y	0.102	0.014
distance	0.108	0.063
GeoSLAM		
x	0.124	0.013
y	0.014	0.05
distance	0.1	0.09

Upon examining the correlation along individual axes and among HMLS devices (Table 6), it is obvious that the correlation value exceeds the significance threshold (0.7) in cases of examining the relationships between the error in the direction of individual axes ($x_{(dif)}$ GeoSLAM and $x_{(dif)}$ Stonex with a value of 0.962 and simultaneously $y_{(dif)}$ GeoSLAM and $y_{(dif)}$ Stonex with a value of 0.93).

Table 6. The correlation coefficient for individual axes and HMLS devices.

	$x_{(dif)}$ **Stonex**	$x_{(dif)}$ **GeoSLAM**	$y_{(dif)}$ **Stonex**	$y_{(dif)}$ **GeoSLAM**
$x_{(dif)}$ Stonex	1	0.962	0.102	0.093
$x_{(dif)}$ GeoSLAM	0.962	1	0.111	0.113
$y_{(dif)}$ Stonex	0.102	0.111	1	0.93
$y_{(dif)}$ GeoSLAM	0.093	0.113	0.93	1

When examining the relationship between position error and thickness error, we aimed to determine whether trees with inaccurately determined positions also exhibit inaccuracies in DBH. However, the correlation between these two variables was not confirmed.

4. Discussion

In this study, we evaluated the performance of GeoSLAM ZEB Horizon and Stonex X120GO SLAM HMLSs addressing two main issues: (i) to assess and compare the results of the positioning achieved based on HMLSs instruments and (ii) to investigate influencing factors and their impact on estimation accuracies. For data collection, the same type of trajectory in five different stand structures were tested. The assessments of tree position and usability of HMLS were satisfying, independent of the device used.

Between March and November 2022, when we collected data, our forests were in the leaf-on season. We assume that the effect of foliage on the quality of the data needs to be investigated, but we also assume that, in our conditions, other important factors, especially the weather (rain and snow), could potentially make data collection impossible. This is especially true in our conditions during the leaf-off season when the wind blows, which could result in more significant challenges when using mobile technologies and, consequently, affect the results adversely.

In the future, we also consider it necessary to investigate the influence of the shape of the terrain on the quality of the subsequent output. In our work, we chose flat terrains because we could examine the effects on the HMLS SLAM technology gradually and later examined the problems in a wider and wider context.

We assume that HMLS SLAM technology, as well as other LIDAR based technologies, can encounter several challenges when scanning on steep slopes; for example, the scanner may have a limited line of sight due to the steep angle, potentially missing parts of the terrain, or the scanner's laser beams may have extremely varying angles of incidence. This can lead to geometric distortions in the data, affecting the accuracy of the point cloud. However, on the other hand, for SLAM technology, this phenomenon might not be a problem; on the contrary, it could be an advantage.

In the FSCT study [49], where a comparison of the manual reference DBH against the automatically extracted measurements was evaluated, RMSE DBH error results were −0.007 m, 0.008 m, and 0.072 m, respectively, and of the 588 reference trees, 535 (90.98%) were successfully detected [49].

The FSCT algorithm was able to match 5141 of the reference diameter measurements fully automatically, with mean, median, and RMSE of 0.032 m, 0.02 m, and 0.103 m, respectively. In previous studies, FSCT offered the advantage of being a robust, sensor-agnostic, and fully automated forest point cloud measurement tool [49]. In a comprehensive exploration of automated extraction for forest parameters at the individual tree level, where a comparison of MLS and TLS applications were performed, 26 of 192 trees were not identified (23.5%). The FSCT algorithm attained RMSE values consistent with the reference measurements for diameter (6 cm) and height (approximately 3 m). These values correspond to 37% of the average height and 26% of the average DBH values in described research [52].

In the case of our study, 417 of 457 trees were successfully detected, conferring a success rate of 91.247%.

4.1. Scanner Type

In terms of control, the GeoSLAM ZEB Horizon utilizes a button directly on the scanner and may require a cable connection to the datalogger and batteries. On the other hand, the Stonex X120GO SLAM is controlled through the GO app, providing a user-friendly interface for scan updates and synchronous display. For GCPs measurement, both scanners are required to stay in a stationary position on the GCP for a few seconds during the scanning process. Post-processing is conducted using GeoSLAM Hub software for the GeoSLAM ZEB Horizon and the GO post 1.0.5 software for the Stonex X120GO SLAM. Ultimately, the choice between these scanners may depend on specific project requirements, preferred control interfaces, and post-processing workflows. In example A (Figure 6), while analyzing an area of a spruce stand with a tree density of 777 trees/ha, Stonex collected 24,829 points in a sample cross-section from the point cloud, whereas GeoSLAM collected 25,625 points. In the overall point cloud, Stonex gathered 24,730,078 points, whereas GeoSLAM obtained 21,458,522 points. In example B (Figure 6), for an area of beech stand with a higher tree density of 1522 trees/ha, Stonex gathered 45,271 points in a sample cross-section from the point cloud, while GeoSLAM collected 44,627 points. In the overall point cloud, Stonex collected 22,957,603 points, whereas GeoSLAM collected 19,944,746 points.

In both examples, Stonex shows a higher number of points in the overall point cloud compared to GeoSLAM. This can be attributed to Stonex's higher data acquisition rate, which allows it to capture more points during scanning. Noise in the point cloud may potentially negatively influence accuracy and reliability for further analysis and applications (Figure 7). Higher noise indicates a lower quality sensor or a different SLAM algorithm approach.

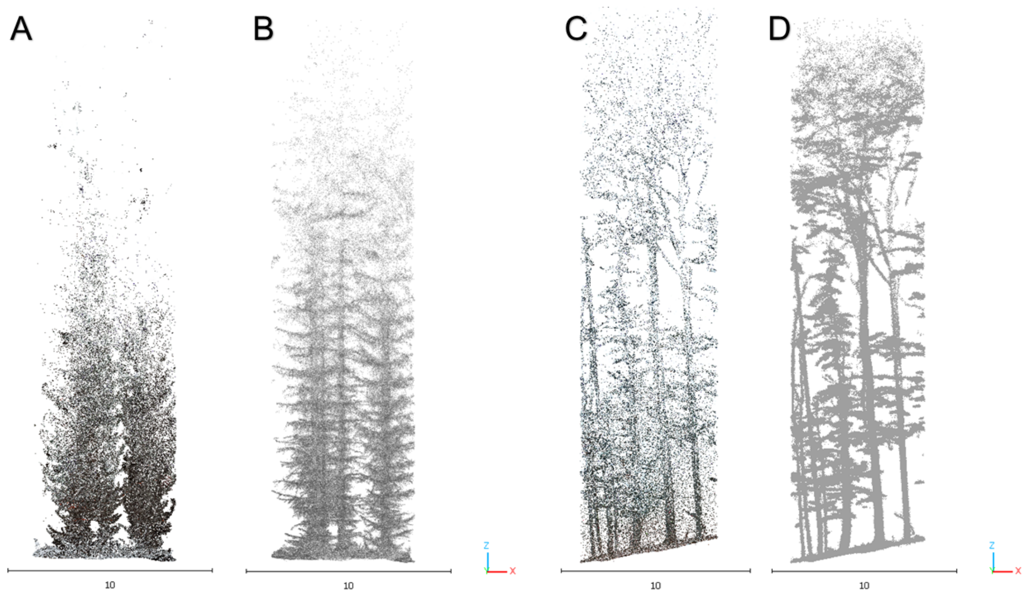

Figure 6. Point cloud visualization: (**A**) Sprue tree stand detail—Stonex HMLS; (**B**) Sprue tree stand detail—GeoSLAM HMLS; (**C**) Beech tree stand detail—Stonex HMLS; (**D**) Beech tree stand detail—GeoSLAM HMLS.

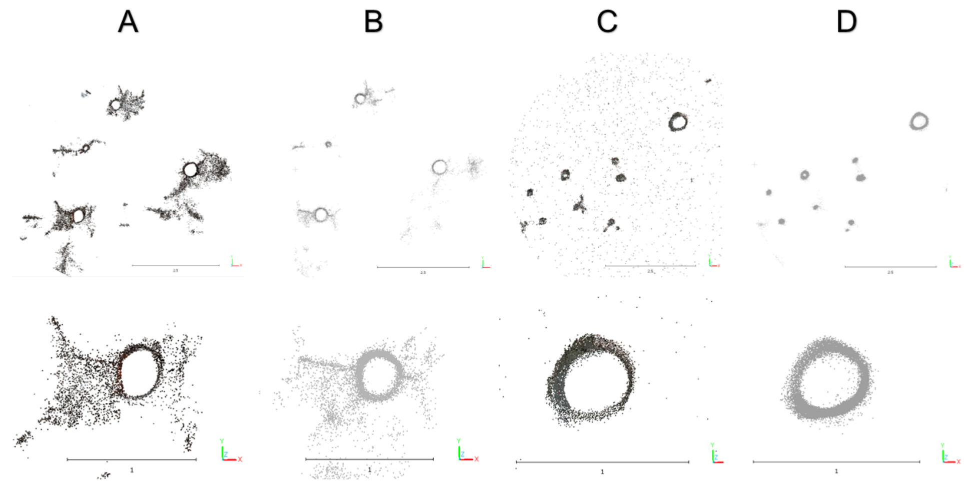

Figure 7. DBH cross-section details (**A**) Sprue tree stand detail—Stonex HMLS; (**B**) Sprue tree stand detail—GeoSLAM HMLS; (**C**) Beech tree stand detail—Stonex HMLS; (**D**) Beech tree stand detail—GeoSLAM HMLS.

Based on our results, the choice of device for similar tasks ultimately rests with the user. However, as this research is in its initial stages, it is essential to explore other potential factors that may influence the results, including foliage, slope, undergrowth, and more. In essence, while there are some differences between the devices, they are not substantial but also not negligible, encompassing aspects such as processing, point cloud quality, and price. In both cases, the devices have not yet undergone extensive testing in a forest environment, and only long-term use will determine their suitability for critical tasks in forest inventory and related fields.

4.2. Data Acquisition Time Assessment

The usability of HMLS in a complex environment has been studied in several studies [22,24,53,54]. In these studies, the authors demonstrated that HMLS mapping in complex environments (forest ecosystems, coastal reefs, etc.) is about forty times faster than using TLS and six times faster than using photo-survey, which is processed with structure from motion and stereo algorithms with multiple views [22]. In addition, it provides evidence of a DBH extraction comparable to the TLS estimate.

With HMLS, authors often evaluate the correctness of determining the strains from the point clouds, which, with HMLS, is up to 90%, since the route is usually planned according to environmental conditions. When compared to TLS and the objects that were scanned with the HMLS ZEB HORIZON in two scan surveys, with different walking speeds the accuracy of tree detection of 96% was investigated [55]. The rate of correct tree trunk detection was 93.3% [53]. In case of this study, the accuracy of tree detection of 96.56% was investigated.

To demonstrate the potential of HMLS with SLAM technology, a comparison with other options in the field of data collection efficiency in a specific environment is necessary. The authors use different methods and procedures, so it is convenient to calculate the area (m^2) versus time (min) for one operator for comparison (Table 7). Depending on the author, various are achieved from 20 m^2 to 277.78 m^2 per min. per operator, when HMLS is compared to TLS, mobile close-range photogrammetry (mCRP) and classic data collection methods [18,22,24,43,47,53,54,56–58]. In this context, mCRP also demonstrates its potential as a fast method of obtaining data that covers an area from 30.63 m^2 to 136 m^2 per min. per operator [57]. The TLS data acquisition rate was lower than the two previous methods (0.85–72.46 m^2 per min per operator) [18,22,24,43,56,58,59]. In the case of this study average acquisition rate was 183.67 m^2/min per surveyor when a total area of 9000 m^2 was captured via HMLS. This method includes a stop at 4 GSPs on each research plot with both HMLS devices (Figure 3).

Table 7. Time consumption of data collection via various methods.

Author	Total Area (m^2)	Method (m^2/min per Surveyor)				
		TLS	HMLS	FS	Reference Data	Positional RMSE (cm)
[22]	780	26	123.81	-	TLS (Riegl VZ-1000)	20.2
[24]	100 500 2500	0.85 - -	20 50 -	- - 0.43	TLS (FARO Focus 3D; 3 scans)	3.1
[18]	225	22.5 3	17.31	7.03	TLS (FARO Focus 3D; 1 and 5 scans)	2.8 ± 14 cm 4.2 ± 7.5 cm
[47]	10,000	51.55	107.53	-	TLS (FARO Focus 3D; 10 scans)	3.5
	5000	72.46	277.78	-	TLS (FARO Focus 3D; 4 scans)	2.4
[56]	531	8.85	75.86	0.74	Field data	9.3
[58]	3500	50	20.83		Field data	20
[54]	25,446	-	217.49	-	HMLS single scan HMLS single scan	9.1 13.9
[53]	300	-	30	0.91	Field data	26
[43]	804 3600	8.29 -	80.4 300	1.04 -	Field data	3.28 1.65
Our research	9000	-	183.67	3.1	Field data	17.91 GeoSLAM 17.33 Stonex

Not all the mentioned studies documented time data on the length of the collection of reference data via total station and GNSS receiver, as it is a series of complex time-consuming activities that must be planned to consider influencing factors such as weather, challenging environment, experienced staff, etc. The average ground-truth data acquisition rate was around the value of 3.1 m^2 per minute per surveyor.

It is important to emphasize that the time of data acquisition is related to the cost of data acquisition, and it is also necessary to consider the cost of acquiring the equipment [60].

4.3. Positional Accuracy

In the application of SLAM technology to the forest environment, research has been moving forward in recent years. Many authors investigate the possibilities of using this technological process in connection with the forest environment and various ecosystems, for example following the work process in the forest and the navigation of mining-transport technologies [11] compared to other mobile laser scanning technologies in boreal forest conditions [61] in the context of mobile robotics, autonomous driving research, and forest operations [62]. As already mentioned, the forest environment is a challenge for many technologies. In recent years, works have been published that also dealt with solving the issue of the location of objects, but most of them were focused on complex integrated systems based on GNSS and INS, which would find their location very difficult in common operations, despite the excellent results (considering the quantum of knowledge that is associated with handling, collection, and overall processing of data, not to mention financial demands). In connection with our research, it is necessary to summarize the works focusing on the problem of localization and mapping in forestry and to summarize the basic characteristics for a more comprehensive overview in the given area. The authors are aware that improving the quality of positional data will also improve the quality of subsequent outputs. For this reason, they are investigating various technological combinations and approaches to determine the location of objects in a challenging environment, but it is necessary to consider the requirements for the accuracy of the location determination and the effort expended.

When the tropical forest tree positioning accuracy was evaluated, and GNSS-enabled smartphones and tablets in data collection were used, the findings indicate that the horizontal positioning accuracy detected by the instruments used in this study were mostly accurate within 5 to 15 m. The RMSEs were higher in the areas surrounded by larger canopy diameter trees [63]. This was to simulate the worst-case scenario when there is absence of Internet or cell phone data coverage. When positioning accuracy of the trajectories of GNSS + IMU and SLAM + IMU were evaluated and the results show that the positioning accuracy in the selected test field was improved by 38% compared to that of a traditional tactical grade IMU + GNSS positioning system in a mature forest environment, the RMSEs 0.52 m and 0.32 were reached [7]. From more recent works, when a portable backpack lidar to measure and locate trees in a nature forest plot was investigated, and the point cloud data and GNSS location records were used the average tree positioning error was 4.64 m [3]. Results were significantly affected by the distance and route length from the measured trees to the data acquisition start position, whereas it was affected little by the habitat complexity and characteristics of tree stems. The research area comprised an area of 10 ha and tree density in the plot was about 8600 trees/ha. The intensive literature review in the area of localization and mapping in agriculture and forestry leads to the main conclusion that only a few methods can achieve simultaneously the desired goals of scalability, availability, and accuracy, due to the challenges imposed by these critical environments [8].

4.3.1. Positional Accuracy HMLS Compared to TLS

SLAM technology in HMLS offers user-friendly alternative to more technologically complex custom-made devices. When evaluating the accuracy of determining the position of trees, we encounter two approaches. The authors compare HMLS data with reference datasets created by the TLS or with field data acquired by classical geodetic approaches (GNSS in combination with a total station). For different approaches and methods, the RMSE varies from 2.4 cm to over 20 cm. When the accuracy of positioning was evaluated at 2500 m^2, the reference TLS data (Faro Focus, 3 scans) were compared with ZEB1. For trees with DBH less than 10 cm study states values RMSE 3.9 cm and for trees with DBH more than 10 cm RMSE was 2.1 cm. Total value reach 2.3 cm and RMSE 3.1 cm [24]. The reference TLS data set (Faro Focus, 3 scans) was compared with ZEB1 on 225 m^2 with Bias 4.2 $\pm$ 7.5 cm for observed trees with DBH up to 10 cm. The azimuth and distance from the plot center represented tree position [64]. HMLS ZEB REVO data were compared with TLS (Faro Focus) data merged/from 10 scans on an area of 10,000 m^2 with the RMSE 3.5 cm [59]. Two types of trajectories compared with a HMLS (ZEB1) single scan at the area of 25,446 m^2 were investigated and reached overall RMSEs of 9.1 and 13.9 cm [54]. Trunk-based SLAM backend for smartphones with online SLAM for large- scale forest inventories was tested; the distance mean between the estimated and reference tree positions was 13.3 cm. The method was tested at 5120 m^2 (in 5 field sample plots (32 $\times$ 32 m^2), and the reference tree positions were collected using TLS through multi-scan method [10].

4.3.2. Positional Accuracy HMLS Compared to Local Coordinate

On research areas with an area of 300 m^2, the overall RMSE of 26 cm was achieved. Reference dataset used the independent coordinate system established by the total station and experimental dataset made by HMLS ZEB-REVO-RT was transform into local coordinate system by four targets [53]. The results show a small difference in the position of the trees. However, it is necessary to pay attention to the reference data used for the accuracy assessment because for many areas of research the position of objects in the real coordinate system is important. Based on the above mentioned, we can see that if TLS (or HMLS) is used as a reference base, positional deviations reach smaller values to than when compared with references obtained by classical geodetical and forest inventory measurement. However, it is necessary to state that if we want to evaluate how accurately we can determine the position of objects from the HMLS clouds in the real coordinate system, the comparison with TLS and the results from it do not have an appropriate informative value because they contain similar errors from postprocessing of the data.

4.3.3. Positional Accuracy HMLS Compared to GNSS

Regarding the comparison of the derived position of the trees with their position in the real coordinate system, we found a smaller number of works than those comparing the outputs of HMLS with TLS. Authors comparing the derived position of objects under the forest canopy with a reference dataset measured on a GNSS basis achieve RMSE values from 4.5 to 20 cm [43,53,56,58]. In our work, overall RMSE was achieved for Stonex 17.33 cm and for GeoSLAM 17.91 cm. The results were achieved by a user-friendly workflow, in which 4 known points on the path of the HMLS device were used for transformation into a coordinate system, all tested in different vegetation conditions. The results, in terms of RMSE (approx. 17 cm), place us in the middle position among other authors with a similar device. When ground truth data were gained by GNSS receiver (plot center), hypsometer for distance and compass for azimuth to each tree, overall RMSE of 9.3 cm, when HMLS was investigated [56]. The area of 3500 m^2 with overall RMSE 20 cm was mapped, tree positions were obtained using the total station and a prism placed in front of the tree center, and the reference tree positions were estimated with a standard deviation of 4.5 cm [58]. In 2015 a SLAM-aided positioning solution with point clouds collected by a small-footprint LiDAR was investigate [7] and the potential of SLAM positioning and mapping in forest inventories was evaluated. The results show that the positioning accuracy of the 224 selected test trees was improved by 38% compared to that of a traditional tactical grade IMU + GNSS positioning system in a mature forest environment. For forest mapping an integrated GNSS/INS/LiDAR-SLAM positioning method was tested in boreal forests at the approximately 800 m long trajectory with 224 trees [12]. Although the horizontal accuracy of the entire trajectory reaches 6 cm, the devices used herein were relatively expensive and displayed better performance.

4.4. Possible Applications of HMLS in Forestry and Precise Positioning

We consider the examination of HMLS outputs also for the purpose of evaluating the accuracy of location determination to be extremely important on an overall scale. With both investigated devices, we were able to achieve results with a positioning error in the real coordinate system of less than 18 cm with relatively simple terrain workflow, at different plot conditions. Based on what is known, the exact position of trees in a forest has several practical uses and benefits, especially in the context of forest management, environmental monitoring, and research, the possibility of exact positional derivation from a device that works very efficiently, and generated outputs are widely applicable, it can be of great benefit to forest practice and development in the field of forest management and nature protection. From the point of view of accurate location determination, there is no significant difference between the examined devices, however, the more expensive GeoSLAM devices provide better quality outputs. The point clouds show less noise, which is a definite advantage, especially in more complex forest structures. However, since the effect of the vegetation and trees density on the accuracy of the location determination has been confirmed, at the same time the positional RMSE is similar for both devices. The final decision regarding the choice of HMLS is on the user which must consider other advantages and disadvantages e.g., user environment, conditions of usage, price. If the lower price and user-friendly simple operation of the device provided by HMLS Stonex are preferred, but at the expense of the quality of the output point cloud, then the more expensive GeoSLAM variant with more powerful sensors and SLAM, which reduce the point clouds noise typical of mobile scanning technologies, would be the better choice.

It is important to note that while specific competitive indexes do not directly involve XY coordinates, there are other spatial analysis techniques and methods in forestry that can use tree coordinates for various purposes. Geographic Information Systems (GIS) can be used to create spatially explicit models to study tree distributions, spatial patterns, and competition across a landscape. Additionally, individual tree mapping data (with extract XY coordinates) can be used to analyze point pattern processes, tree clustering, and spatial relationships between trees. Spatial Point Pattern Analysis, method used to study the structural arrangement of individual trees within a forest stand helped to identify patterns like clustering, regularity, or randomness, which can provide insights into natural regeneration, competition, and other ecological processes, and directly involve XY coordinates [65]. Precise positioning improves interpolation methods used to estimate values of forest attributes (e.g., tree height, species composition) at unsampled locations based on data from sampled locations effectively collected via HMLSs [66].

Knowledge about the exact location of individuals helps identify areas with similar characteristics and can assist in zoning for specific management strategies (spatial autocorrelation [67–70]) or helps understand the fragmentation or connectivity of forest patches, which is crucial for wildlife habitat assessment and biodiversity conservation (patch analysis [71–73]). The exact positions of the trees will find their application in the creation of digital twins or in modeling, or as an input to growth simulators, too. It is evident that the variations in HMLSs results are not significant; instead, distinctions arise in equipment handling, data processing, and the quality of point clouds. Consequently, the choice of device for a similar task ultimately rests with the user.

The paper describes the beginning phase of a long-term research project, focusing on investigating additional factors that we anticipate will influence the outcomes. These factors include foliage, slope, and undergrowth. We are comparing a device with a long-standing presence in the market with a relative newcomer in the field. Nonetheless, predicting the future of HMLS usage in forestry remains challenging.

Just as it is possible to discuss the rapid development of electronic devices and their fast obsolescence, there is also an assumption that HMLS, thanks to their advantages, can be applied in practice and move the collection of detailed data for forest inventory to a new level.

5. Conclusions

Accurate tree positioning data is vital for informed decisions about land use, conservation, and sustainable management. It enhances measurement precision under forest cover, improving mapping and subsequent data processing for both scientific research and forestry practice.

The study's significant advantage lies in its unique comparison of two HMLS devices, exploring their precision and limitations in forest environments—an area largely unexplored in previous research.

The study outlines the methodological procedures for HMLS data collection using the GeoSLAM ZEB Horizon and Stonex X120GO SLAM devices as alternative approaches. The goal is to assess the accuracy of locating objects recorded beneath the forest canopy, as automatically derived from these devices' outputs. The advantage of comparing two HMLS devices in a challenging environment is a comprehensive assessment of each device's performance and capabilities under difficult conditions. This can aid users in making informed decisions about which device suits their specific needs best.

The positional RMSE was 17.33 cm for Stonex and 17.91 cm for GeoSLAM across various forest types, considering species composition and density. The research confirms that tree species and forest density influence positioning accuracy. Additionally, the analysis reveals a weak association between tree distance from the HMLS trajectory and positioning error. These results demonstrate that HMLS accuracy is sufficient for deriving tree and forest parameters with satisfactory precision. GeoSLAM HMLS performs better than Stonex for larger distances, which provides valuable insights for selecting the appropriate data collection method based on required accuracy and distance range.

However, it's worth noting that while Stonex HMLS has low positional error, its point cloud may contain more noise, posing challenges in young stands with branches close to the trunk base. In contrast, it works well in older stands, but issues may arise in areas with undergrowth or taller herbaceous vegetation.

This study could help determine the value for money each device offers, allowing users to balance cost against performance in demanding scenarios. Overall, this testing of two commonly used HMLS devices in challenging environments could enhance our understanding of their real-world applicability and limitations.

Author Contributions: Conceptualization, J.C. and J.V.; methodology, J.C., J.V. and J.T. (Julián Tomaštík); formal analysis, J.V.; investigation, J.C., J.V., F.C., D.T. and M.S.; data curation, J.C.; writing—original draft preparation, J.C.; writing—review and editing, J.V., J.T. (Julián Tomaštík) and M.M.; visualization, J.C.; supervision, J.T. (Ján Tuček) and F.C.; project administration, J.V. and M.M.; funding acquisition, J.V. and M.M. All authors have read and agreed to the published version of the manuscript.

Funding: This research was funded by the Slovak Research and Development Agency under Contract No. APVV-20-0391 (Monitoring of forest stands in three-dimensional space and time by innovative close-range approaches).

Data Availability Statement: The data presented in this study are available on request from the corresponding author. The data are not publicly available due to the large volume of data.

Conflicts of Interest: The authors declare no conflicts of interest. The individuals appearing in the images gave consent for their faces to appear in published materials.

References

1. Bettinger, P.; Merry, K.; Bayat, M.; Tomaštík, J. GNSS use in forestry—A multi-national survey from Iran, Slovakia and southern USA. *Comput. Electron. Agric.* **2019**, *158*, 369–383. [CrossRef]
2. Yuan, F.; Chen, S.; Fang, L.; Zheng, S.; Liu, Y.; Ren, J. A Method to Locate Tree Positions Using Ultrawideband Technology. *J. Sensors* **2021**, *2021*, 5539302. [CrossRef]
3. Xie, Y.; Yang, T.; Wang, X.; Chen, X.; Pang, S.; Hu, J.; Wang, A.; Chen, L.; Shen, Z. Applying a Portable Backpack Lidar to Measure and Locate Trees in a Nature Forest Plot: Accuracy and Error Analyses. *Remote Sens.* **2022**, *14*, 1806. [CrossRef]

4. Von Gadow, K.; Hui, G.Y. Characterizing forest spatial structure and diversity. *Proc. SUFOR Int. Work. Sustain. For. Temp. Reg.* **2002**, 20–30.
5. Liu, J.; Feng, Z.; Mannan, A.; Yang, L. Positioning of coordinates and precision analysis of sample trees using the intelligent forest survey calculator. *Comput. Electron. Agric.* **2019**, *159*, 157–164. [CrossRef]
6. Kaartinen, H.; Hyyppä, J.; Kukko, A.; Jaakkola, A.; Hyyppä, H. Benchmarking the performance of mobile laser scanning systems using a permanent test field. *Sensors* **2012**, *12*, 12814–12835. [CrossRef]
7. Tang, J.; Chen, Y.; Kukko, A.; Kaartinen, H.; Jaakkola, A.; Khoramshahi, E.; Hakala, T.; Hyyppä, J.; Holopainen, M.; Hyyppä, H. SLAM-Aided Stem Mapping for Forest Inventory with Small-Footprint Mobile LiDAR. *Forests* **2015**, *6*, 4588–4606. [CrossRef]
8. Aguiar, A.S.; Dos Santos, F.N.; Cunha, J.B.; Sobreira, H.; Sousa, A.J. Localization and mapping for robots in agriculture and forestry: A survey. *Robotics* **2020**, *9*, 97. [CrossRef]
9. Chahine, G.; Vaidis, M.; Pomerleau, F.; Pradalier, C.C. Mapping in unstructured natural environment: A sensor fusion framework for wearable sensor suites. *SN Appl. Sci.* **2021**, *3*, 571. [CrossRef]
10. Fan, Y.; Feng, Z.; Shen, C.; Khan, T.U.; Mannan, A.; Gao, X.; Chen, P.; Saeed, S. A trunk-based SLAM backend for smartphones with online SLAM in large-scale forest inventories. *ISPRS J. Photogramm. Remote Sens.* **2020**, *162*, 41–49. [CrossRef]
11. Nevalainen, P.; Li, Q.; Melkas, T.; Riekki, K.; Westerlund, T.; Heikkonen, J. Navigation and mapping in forest environment using sparse point clouds. *Remote Sens.* **2020**, *12*, 4088. [CrossRef]
12. Qian, C.; Liu, H.; Tang, J.; Chen, Y.; Kaartinen, H.; Kukko, A.; Zhu, L.; Liang, X.; Chen, L.; Hyyppä, J. An integrated GNSS/INS/LiDAR-SLAM positioning method for highly accurate forest stem mapping. *Remote Sens.* **2017**, *9*, 3. [CrossRef]
13. Abellanas, B.; Pérez-Moreno, P. Assessing spatial dynamics of a Pinus nigra subsp. salzmannii natural stand combining point and polygon patterns analysis. *For. Ecol. Manag.* **2018**, *424*, 136–153. [CrossRef]
14. Brovkina, O.; Cienciala, E.; Surový, P.; Janata, P. Unmanned aerial vehicles (UAV) for assessment of qualitative classification of Norway spruce in temperate forest stands. *Geo-Spat. Inf. Sci.* **2018**, *21*, 12–20. [CrossRef]
15. Chamagne, J.; Tanadini, M.; Frank, D.; Matula, R.; Paine, C.E.T.; Philipson, C.D.; Svátek, M.; Turnbull, L.A.; Volařík, D.; Hector, A. Forest diversity promotes individual tree growth in central European forest stands. *J. Appl. Ecol.* **2017**, *54*, 71–79. [CrossRef]
16. Cienciala, E.; Tumajer, J.; Zatloukal, V.; Beranová, J.; Holá, Š.; Hůnová, I.; Russ, R. Recent spruce decline with biotic pathogen infestation as a result of interacting climate, deposition and soil variables. *Eur. J. For. Res.* **2017**, *136*, 307–317. [CrossRef]
17. Mokroš, M.; Mikita, T.; Singh, A.; Tomaštík, J.; Chudá, J.; Wężyk, P.; Kuželka, K.; Surový, P.; Klimánek, M.; Zięba-Kulawik, K.; et al. Novel low-cost mobile mapping systems for forest inventories as terrestrial laser scanning alternatives. *Int. J. Appl. Earth Obs. Geoinf.* **2021**, *104*, 102512. [CrossRef]
18. Bauwens, S.; Bartholomeus, H.; Calders, K.; Lejeune, P. Forest Inventory with Terrestrial LiDAR: A Comparison of Static and Hand-Held Mobile Laser Scanning. *Forests* **2016**, *7*, 127. [CrossRef]
19. Holopainen, M.; Kankare, V.; Vastaranta, M.; Liang, X.; Lin, Y.; Vaaja, M.; Yu, X.; Hyyppä, J.; Hyyppä, H.; Kaartinen, H.; et al. Tree mapping using airborne, terrestrial and mobile laser scanning—A case study in a heterogeneous urban forest. *Urban For. Urban Green.* **2013**, *12*, 546–553. [CrossRef]
20. Chen, Y.; Tang, J.; Jiang, C.; Zhu, L.; Lehtomäki, M.; Kaartinen, H.; Kaijaluoto, R.; Wang, Y.; Hyyppä, J.; Hyyppä, H.; et al. The Accuracy Comparison of Three Simultaneous Localization and Mapping (SLAM)-Based Indoor Mapping Technologies. *Sensors* **2018**, *18*, 3228. [CrossRef]
21. Durrant-Whyte, H.; Bailey, T. Simultaneous localization and mapping: Part I. *IEEE Robot. Autom. Mag.* **2006**, *13*, 99–110. [CrossRef]
22. James, M.R.; Quinton, J.N. Ultra-rapid topographic surveying for complexenvironments: The hand-held mobile laser scanner(HMLS). *Earth Surf. Process. Landf.* **2014**, *39*, 138–142. [CrossRef]
23. Bienert, A.; Maas, H.; Scheller, S. Analysis of the information content of terrestrial laserscanner point clouds for the automatic determination of forest inventory parameters. *Work. 3D Remote Sens. For.* **2006**, *14*, 1–7.
24. Ryding, J.; Williams, E.; Smith, M.J.; Eichhorn, M.P. Assessing handheld mobile laser scanners for forest surveys. *Remote Sens.* **2015**, *7*, 1095–1111. [CrossRef]
25. Yadav, M.; Singh, A.K.; Lohani, B. Computation of road geometry parameters using mobile LiDAR system. *Remote Sens. Appl. Soc. Environ.* **2018**, *10*, 18–23. [CrossRef]
26. Croser, J. A handy device. *Land J.* **2016**, *22*, 2015–2017.
27. Makkonen, T.; Heikkilä, R.; Kaaranka, A.; Naatsaari, M. The applicability of the rapid handheld laser scanner to underground tunnel surveying. In Proceedings of the 32nd International Symposium on Automation and Robotics in Construction Mining: Connected to the Future, Oulu, Finland, 15–18 June 2015. [CrossRef]
28. Tomaštík, J.; Saloň, Š.; Tunák, D.; Chudý, F.; Kardoš, M. Tango in forests—An initial experience of the use of the new Google technology in connection with forest inventory tasks. *Comput. Electron. Agric.* **2017**, *141*, 109–117. [CrossRef]
29. Hyyppä, J.; Virtanen, J.-P.; Jaakkola, A.; Yu, X.; Hyyppä, H.; Liang, X. Feasibility of Google Tango and Kinect for Crowdsourcing Forestry Information. *Forests* **2018**, *9*, 6. [CrossRef]
30. Draelos, M.; Qiu, Q.; Bronstein, A.; Sapiro, G. Intel realsense = Real low cost gaze. In Proceedings of the 2015 IEEE International Conference on Image Processing (ICIP), Québec City, QC, Canada, 27–30 September 2015; pp. 2520–2524.
31. Taheri, H.; Xia, Z.C. SLAM; definition and evolution. *Eng. Appl. Artif. Intell.* **2021**, *97*, 104032. [CrossRef]

32. Winberg, O.; Pyörälä, J.; Yu, X.; Kaartinen, H.; Kukko, A.; Holopainen, M.; Holmgren, J.; Lehtomäki, M.; Hyyppä, J. Branch information extraction from Norway spruce using handheld laser scanning point clouds in Nordic forests. *ISPRS Open J. Photogramm. Remote Sens.* **2023**, *9*, 100040. [CrossRef]
33. Eker, R. Comparative use of PPK-integrated close-range terrestrial photogrammetry and a handheld mobile laser scanner in the measurement of forest road surface deformation. *Measurement* **2023**, *206*, 112322. [CrossRef]
34. Del Duca, G.; Machado, C. Assessing the Quality of the Leica BLK2GO Mobile Laser Scanner versus the Focus 3D S120 Static Terrestrial Laser Scanner for a Preliminary Study of Garden Digital Surveying. *Heritage* **2023**, *6*, 1007–1027. [CrossRef]
35. Tupinambá-Simões, F.; Pascual, A.; Guerra-Hernández, J.; Ordóñez, C.; de Conto, T.; Bravo, F. Assessing the Performance of a Handheld Laser Scanning System for Individual Tree Mapping & mdash; A Mixed Forests Showcase in Spain. *Remote Sens.* **2023**, *15*, 1169.
36. Yiğit, A.Y.; Hamal, S.N.; Yakar, M.; Ulvi, A. Investigation and Implementation of New Technology Wearable Mobile Laser Scanning (WMLS) in Transition to an Intelligent Geospatial Cadastral Information System. *Sustainability* **2023**, *15*, 7159. [CrossRef]
37. Tanduo, B.; Losè, L.T.; Chiabrando, F. Documentation of Complex Environments in Cultural Heritage Sites. a Slam-Based Survey in the Castello Del Valentino Basement. *Int. Arch. Photogramm. Remote Sens. Spat. Inf. Sci.-ISPRS Arch.* **2023**, *48*, 489–496. [CrossRef]
38. Martino, A.; Breggion, E.; Balletti, C.; Guerra, F.; Renghini, G.; Centanni, P. Digitization Approaches for Urban Cultural Heritage: Last Generation Mms Within Venice Outdoor Scenarios. *Int. Arch. Photogramm. Remote Sens. Spat. Inf. Sci.-ISPRS Arch.* **2023**, *48*, 265–272. [CrossRef]
39. Stăncioiu, P.T.; Dutcă, I.; Florea, S.C.; Paraschiv, M. Measuring Distances and Areas under Forest Canopy Conditions—A Comparison of Handheld Mobile Laser Scanner and Handheld Global Navigation Satellite System. *Forests* **2022**, *13*, 1893.
40. Ulvi, A.; Yiugit, A.Y. Comparison of the Wearable Mobile Laser Scanner (WMLS) with Other Point Cloud Data Collection Methods in Cultural Heritage: A Case Study of Diokaisareia. *J. Comput. Cult. Herit.* **2022**, *15*, 1–19. [CrossRef]
41. Qi, Y.; Coops, N.C.; Daniels, L.D.; Butson, C.R. Comparing tree attributes derived from quantitative structure models based on drone and mobile laser scanning point clouds across varying canopy cover conditions. *ISPRS J. Photogramm. Remote Sens.* **2022**, *192*, 49–65. [CrossRef]
42. Vandendaele, B.; Martin-Ducup, O.; Fournier, R.A.; Pelletier, G.; Lejeune, P. Mobile Laser Scanning for Estimating Tree Structural Attributes in a Temperate Hardwood Forest. *Remote Sens.* **2022**, *14*, 4522. [CrossRef]
43. Chudá, J.; Hunčaga, M.; Tuček, J.; Mokroš, M. The Handheld Mobile Laser Scanners as a Tool For Accurate Positioning Under Forest Canopy. *ISPRS-Int. Arch. Photogramm. Remote Sens. Spat. Inf. Sci.* **2020**, *XLIII-B1-2*, 211–218. [CrossRef]
44. Hackenberg, J.; Spiecker, H.; Calders, K.; Disney, M.; Raumonen, P. SimpleTree—An Efficient Open Source Tool to Build Tree Models from TLS Clouds. *Forests* **2015**, *6*, 4245–4294. [CrossRef]
45. Ravaglia, J.; Fournier, R.A.; Bac, A.; Véga, C.; Côté, J.-F.; Piboule, A.; Rémillard, U. Comparison of Three Algorithms to Estimate Tree Stem Diameter from Terrestrial Laser Scanner Data. *Forests* **2019**, *10*, 599. [CrossRef]
46. Trochta, J.; Krůček, M.; Vrška, T.; Král, K. 3D Forest: An application for descriptions of three-dimensional forest structures using terrestrial LiDAR. *PLoS ONE* **2017**, *12*, e0176871. [CrossRef]
47. Cabo, C.; Ordóñez, C.; López-Sánchez, C.A.; Armesto, J. Automatic dendrometry: Tree detection, tree height and diameter estimation using terrestrial laser scanning. *Int. J. Appl. Earth Obs. Geoinf.* **2018**, *69*, 164–174. [CrossRef]
48. Koreň, M. DendroCloud User Guide: Version1.49. 2019. Available online: https://gis.tuzvo.sk/dendrocloud/default.aspx (accessed on 17 February 2023).
49. Krisanski, S.; Taskhiri, M.S.; Aracil, S.G.; Herries, D.; Muneri, A.; Gurung, M.B.; Montgomery, J.; Turner, P. Forest structural complexity tool—An open source, fully-automated tool for measuring forest point clouds. *Remote Sens.* **2021**, *13*, 4677. [CrossRef]
50. Ostertagová, E.; Ostertag, O.; Kováč, J. Methodology and application of the Kruskal-Wallis test. *Appl. Mech. Mater.* **2014**, *611*, 115–120. [CrossRef]
51. Sedgwick, P. Pearson's correlation coefficient. *BMJ* **2012**, *345*, e4483. [CrossRef]
52. Spadavecchia, C.; Belcore, E.; Grasso, N.; Piras, M. A Fully Automatic Forest Parameters Extraction At Single-Tree Level: A Comparison of Mls and Tls Applications. *Int. Arch. Photogramm. Remote Sens. Spat. Inf. Sci.-ISPRS Arch.* **2023**, *48*, 457–463. [CrossRef]
53. Chen, S.; Liu, H.; Feng, Z.; Shen, C.; Chen, P. Applicability of personal laser scanning in forestry inventory. *PLoS ONE* **2019**, *14*, e0211392. [CrossRef]
54. Del Perugia, B.; Giannetti, F.; Chirici, G.; Travaglini, D.; Del Perugia, B.; Giannetti, F.; Chirici, G.; Travaglini, D. Influence of Scan Density on the Estimation of Single-Tree Attributes by Hand-Held Mobile Laser Scanning. *Forests* **2019**, *10*, 277. [CrossRef]
55. Gollob, C.; Ritter, T.; Nothdurft, A. Forest inventory with long range and high-speed Personal Laser Scanning (PLS) and Simultaneous Localization and Mapping (SLAM) technology. *Remote Sens.* **2020**, *12*, 1509. [CrossRef]
56. Giannetti, F.; Puletti, N.; Quatrini, V.; Travaglini, D.; Bottalico, F.; Corona, P.; Chirici, G. Integrating terrestrial and airborne laser scanning for the assessment of single-tree attributes in Mediterranean forest stands. *Eur. J. Remote Sens.* **2018**, *51*, 795–807. [CrossRef]
57. Mokro, M.; Liang, X.; Surový, P.; Valent, P.; Čerňava, J.; Chudý, F.; Tunák, D.; Saloň, I.; Merganič, J. Evaluation of close-Range photogrammetry image collection methods for estimating tree diameters. *ISPRS Int. J. Geo-Inf.* **2018**, *7*, 93. [CrossRef]

58. Oveland, I.; Hauglin, M.; Giannetti, F.; Schipper Kjørsvik, N.; Gobakken, T. Comparing Three Different Ground Based Laser Scanning Methods for Tree Stem Detection. *Remote Sens.* **2018**, *10*, 538. [CrossRef]
59. Cabo, C.; Del Pozo, S.; Rodríguez-Gonzálvez, P.; Ordóñez, C.; González-Aguilera, D. Comparing terrestrial laser scanning (TLS) and wearable laser scanning (WLS) for individual tree modeling at plot level. *Remote Sens.* **2018**, *10*, 540. [CrossRef]
60. Hunčaga, M.; Chudá, J.; Tomaštík, J.; Slámová, M.; Koreň, M.; Chudý, F. The comparison of stem curve accuracy determined from point clouds acquired by different terrestrial remote sensing methods. *Remote Sens.* **2020**, *12*, 2739. [CrossRef]
61. Hyyppä, E.; Kukko, A.; Kaijaluoto, R.; White, J.C.; Wulder, M.A.; Pyörälä, J.; Liang, X.; Yu, X.; Wang, Y.; Kaartinen, H.; et al. Accurate derivation of stem curve and volume using backpack mobile laser scanning. *ISPRS J. Photogramm. Remote Sens.* **2020**, *161*, 246–262. [CrossRef]
62. Ali, I.; Durmush, A.; Suominen, O.; Yli-Hietanen, J.; Peltonen, S.; Collin, J.; Gotchev, A. FinnForest dataset: A forest landscape for visual SLAM. *Rob. Auton. Syst.* **2020**, *132*, 103610. [CrossRef]
63. Fauzi, M.F.; Idris, N.H.; Yahya, M.H.; Din, A.H.M.; Idris, N.H.; Lau, A.M.S.; Ishak, M.H.L. Tropical forest tree positioning accuracy: A comparison of low cost GNSS-enabled devices. *Int. J. Geoinform.* **2016**, *12*, 59–66.
64. Bauwens, S.; Fayolle, A.; Gourlet-Fleury, S.; Ndjele, L.M.; Mengal, C.; Lejeune, P. Terrestrial photogrammetry: A non-destructive method for modelling irregularly shaped tropical tree trunks. *Methods Ecol. Evol.* **2017**, *8*, 460–471. [CrossRef]
65. Ben-Said, M. Spatial point-pattern analysis as a powerful tool in identifying pattern-process relationships in plant ecology: An updated review. *Ecol. Process.* **2021**, *10*, 56. [CrossRef]
66. Li, B.; Shi, X.; Zhu, A.X.; Wang, C.; Lin, H. *New Thinking in GIScience*; Springer: Singapore, 2022; ISBN 9789811938160.
67. Getis, A. Spatial Pattern Analysis. In *Encyclopedia of Social Measurement*; Kempf-Leonard, K., Ed.; Elsevier: New York, NY, USA, 2005; pp. 627–632. ISBN 978-0-12-369398-3.
68. Li, J.; He, J.; Liu, Y.; Wang, D.; Rafay, L.; Chen, C.; Hong, T.; Fan, H.; Lin, Y. Spatial Autocorrelation Analysis of Multi-Scale Damaged Vegetation in the Wenchuan Earthquake-Affected Area, Southwest China. *Forests* **2019**, *10*, 195. [CrossRef]
69. Wong, D.W.S.; Wang, F. *Spatial Analysis Methods*; Elsevier: Amsterdam, The Netherlands, 2017; Volume 3, ISBN 9780128046609.
70. Xu, Q.; Li, B.; McRoberts, R.E.; Li, Z.; Hou, Z. Harnessing data assimilation and spatial autocorrelation for forest inventory. *Remote Sens. Environ.* **2023**, *288*, 113488. [CrossRef]
71. Kundu, K.; Halder, P.; Mandal, J.K. Change Detection and Patch Analysis of Sundarban Forest During 1975–2018 Using Remote Sensing and GIS Data. *SN Comput. Sci.* **2021**, *2*, 364. [CrossRef]
72. Paudel, S.; Yuan, F. Assessing landscape changes and dynamics using patch analysis and GIS modeling. *Int. J. Appl. Earth Obs. Geoinf.* **2012**, *16*, 66–76. [CrossRef]
73. Yevide, S.I.A.; Cobbina, N.D.; Loescher, H.W.; Khan, A.S.; Baffoe, A. Land use change and forest patch analysis as a decision-making tool to sustainably develop plantation agriculture and optimize biodiversity conservation. *Afr. J. Ecol.* **2023**, *61*, 675–688. [CrossRef]

Disclaimer/Publisher's Note: The statements, opinions and data contained in all publications are solely those of the individual author(s) and contributor(s) and not of MDPI and/or the editor(s). MDPI and/or the editor(s) disclaim responsibility for any injury to people or property resulting from any ideas, methods, instructions or products referred to in the content.